Available online at www.sciencedirect.com

SCIENCE DIRECT®

Journal of Nuclear Materials 337–339 (2005) 677–683

journal of nuclear materials

www.elsevier.com/locate/jnucmat

Edge localized modes control: experiment and theory

M. Becoulet [a,*], G. Huysmans [a], P. Thomas [a], E. Joffrin [a], F. Rimini [a], P. Monier-Garbet [a], A. Grosman [a], P. Ghendrih [a], V. Parail [b], P. Lomas [b], G. Matthews [b], H. Wilson [b], M. Gryaznevich [b], G. Counsell [b], A. Loarte [c], G. Saibene [c], R. Sartori [c], A. Leonard [d], P. Snyder [d], T. Evans [d], P. Gohil [d], R. Moyer [e], Y. Kamada [f], N. Oyama [f], T. Hatae [f], K. Kamiya [f], A. Degeling [g], Y. Martin [g], J. Lister [g], J. Rapp [h], C. Perez [h], P. Lang [i], A Chankin [i], T. Eich [i], A. Sips [i], J. Stober [i], L. Horton [i], A. Kallenbach [i], W. Suttrop [i], S. Saarelma [j], S. Cowley [k], J. Lönnroth [l], M. Shimada [m], A. Polevoi [m], G. Federici [n]

[a] *Association Euratom-CEA, CEA Cadarache, DSM/DRFC, F-13108 St. Paul-lez-Durance, France*
[b] *Euratom/UKAEA Association, Fusion Culham Science Centre, Abingdon, OX14 3EA, UK*
[c] *EFDA Close Support Unit, 2 Boltzmannstrasse, D-85748 Garching, Germany*
[d] *General Atomics, 3550 General Atomics Court, P.O. Box 85608 San Diego, CA, USA*
[e] *University of California, San Diego, La Jolla CA 92093,USA*
[f] *Japan Atomic Energy Research Institute (JAERI), 801-1 Mukoyama, Naka-machi, Naka-gun 311-0193, Japan*
[g] *Centre de Recherches en Physique des Plasmas, Association Euratom-Confédération Suisse, Ecole Polytechnique Fédérale de Lausanne,CH-1015 Lausanne, Switzerland*
[h] *Institut für Plasmaphysik, Forschungszentrum Jülich, D-52425 Jülich, Germany*
[i] *Association Euratom-IPP, MPI für Plasmaphysik, 2 Boltzmannstrasse, Garching, D-85748, Germany*
[j] *Helsinki University of Technology, Euratom-TEKES Association, FIN-02015 HUT, Finland*
[k] *Department of Physics, Imperial College, Prince Consort Road, London, SW7 2BZ, UK*
[l] *Euratom-Tekes, Helsinki University of Technology, P.O. Box 2200, 02015 HUT, Finland*
[m] *ITER International Team, Mukouyama, Naka-machi, Naka-gun, Ibaraki-ken 311-0193, Japan*
[n] *ITER JWS Garching Co-center, Boltzmannstrae2, 85748 Garching, Germany*

Abstract

The paper reviews recent theoretical and experimental results focussing on the identification of the key factors controlling ELM energy and particle losses both in natural ELMs and in the presence of external controlling mechanisms. Present experiment and theory pointed out the benefit of the high plasma shaping, high q_{95} and high pedestal density in reducing the ELM affected area and conductive energy losses in Type I ELMs. Small benign ELMs regimes in present machines (EDA, HRS, Type II, Grassy, QH, Type III in impurity seeded discharges at high δ) and their relevance for

* Corresponding author. Tel.: +33 4 42257484; fax: +33 4 42254990.
E-mail address: marina@drfc.cad.cea.fr (M. Becoulet).

0022-3115/$ - see front matter
doi:10.1016/j.jnucmat.2004.09.074

ITER are reviewed. Recent studies of active control of ELMs using stochastic boundaries, small pellets and edge current generation are presented.

PACS: 50.55.Fa; 52.35.Py
Keywords: ELM; ELM control; Edge modelling

1. Introduction

Edge Localised Modes (ELM) represent Magneto Hydro Dynamics (MHD) instabilities in the pedestal region typical for H-mode scenarios [1–4]. They provide burst-like energy and particle transport through the external transport barrier (ETB) on a fast MHD time scale in a quasi-periodic way followed by a phase of the pedestal pressure profile rebuilding. The strong link between the maximum achievable plasma confinement and ELM regimes is well established in present tokamaks [3,5–7]. In particular, the most studied Type I ELMs correspond to the high confinement H-mode scenario foreseen for ITER [8]. At the same time energy losses in Type I ELMs in ITER can be problematic for the divertor target plates leading to melting, erosion, and evaporation of proposed divertor materials [9]. According to the present erosion estimates for carbon and tungsten divertor plates, the acceptable lifetime for the target ($>10^6$ Type I ELMs,) can be achieved if the energy loss from the pedestal per ELM does not exceed 5 MJ–14 MJ. Due to the large uncertainties in the previous extrapolations and to the statistical properties of Type I ELMs themselves [10] the predictions for ITER still remain an open question, but are still too marginal to be optimistic, motivating the present study of Type I ELMs control.

Type III ELM regimes are usually observed at lower input power as compared to Type I regimes or at high density [7] and are characterized by high frequency and acceptably small energy losses per ELM. But at the same time the poor confinement of such regimes is not sufficient for a standard H-mode scenario in ITER [8]. A recent investigation of high triangularity impurity seeded (N_2) discharges in JET suggests the possibility of an H-mode scenario with Type III ELMs for ITER with the reference plasma current increased to 17 MA [11]. However, impurity injection to enhance divertor radiation is a questionable technique because of the potential for their accumulation in the plasma.

The possible combination of high confinement (close to Type I ELMs regimes) H-modes and small benign edge MHD activity instead of large energy bursts was demonstrated in many tokamaks in specific plasma conditions. However, Grassy ELMs [12], Type II regimes [13,14], EDA [15], HRS [16], QH mode [17] have been obtained in a narrow operational windows that do not match ITER parameters [4]. Some of these small ELM regimes can be combined with improved core confinement [18,19,16,20,21] but still their extrapolation to ITER is an open question.

The present situation has motivated recent experimental and theoretical development of active ELMs control using externally imposed control mechanisms. In particular stochastic boundaries [22–25], small pellets [26], edge electromagnetic ELM triggering by vertical plasma displacements in an inhomogeneous magnetic field [27], and in plasma current ramp experiments [4,7,22] were tried as ELM control tools.

The paper reviews recent theoretical and experimental results focussing on the identification of the key factors controlling ELM energy and particle losses for natural and externally induced ELMs. The recent results of an ideal linear MHD stability analysis, non-linear explosive evolution of ballooning modes and transport modelling with Type I ELMs are presented in Section 2. In Section 3 the convective and conductive losses behaviour is discussed with respect to the changes in triangularity, q_{95} factor, density, and collisionality. In particular conditions the burst-like transport in Type I ELMs can be replaced by a more continuous (in time) edge MHD activity providing increased transport through ETB. These benign ELMs regimes in present tokamaks and their operational domains are presented briefly. Section 4. revises presently known techniques of active ELMs control such as edge ergodisation by external coils, pellets and edge current generation using plasma current ramps and vertical oscillations of plasma column. Conclusions are presented in Section 5.

2. Progress in theory

The most dangerous for the ITER divertor are Type I ELMs which have similar characteristics in all tokamaks. In particular the temperature and density crash first on the low field side (LFS) as seen on many diagnostics suggests the presence of the ballooning like instability [28–32]. The characteristic time of the pedestal crash ($\sim$ 200–300 μs) and the MHD signature observed on the magnetic probes are also similar [4,10]. There is also a large amount of experimental evidence of the bursty nature of ELM induced perpendicular transport in the SOL [33,34].

The destabilisation of the peeling and ballooning modes driven by the edge parallel current density (mainly by the large bootstrap current fraction), and the edge pressure gradient respectively, are considered presently as candidates for Type I ELM triggers [1,35–38]. The development of the ideal linear MHD stability codes for ballooning and peeling modes and their confrontation of experimental data suggests that the main mechanism of Type I ELMs has been identified. For example, the maximum achievable pedestal pressure in experimental Type I ELMs regimes correspond to the calculated ideal MHD limit for coupled ballooning-peeling modes [36]. The improvement of the pedestal confinement with plasma shaping (triangularity) was demonstrated in many machines [5,12–14] and was also explained by MHD stability calculations. The improvement of edge stability is attributed to the increased magnetic shear and the possible access to the second stability regime at high triangularity [36,39–41]. All these facts give confidence in the stability calculations for ITER [36]. The pedestal width scaling for ITER remains the main uncertainty. However, with reasonable assumptions for ITER pedestal parameters, one can expect the ideal coupled ballooning-peeling mode destabilisation and hence Type I ELMs.

Linear codes are limited in the description of the ELM dynamics. A recently proposed non-linear model suggests that ballooning modes can develop explosively, giving birth to narrow fingerlike structures pushing aside other field lines and spreading the instability over a large plasma region [42], demonstrating a qualitative agreement with experiment [35]. 3D non-linear calculations with BOUT-code [43] also suggest the bursty transport to the SOL due to ballooning modes at least in the early non-linear stage [36]. For the moment this image of Type I ELMs is not developed far enough to reproduce ELM cycles.

1,5D transport modelling with ELMs [41,44,45] is based on the assumption that the transport coefficients in the ELM affected area are increased proportionally to the unstable modes amplitudes suggested by the linear ideal MHD theory. These transport models reproduce the ELM cycle, but they contain adhoc parameters to match experimental ELM time and size.

A similar ideology for a growth rate calculation for ballooning modes is adapted in the 2D transport code TELM [4] which is coupled with the ideal MHD code MISHKA [37]. The difference to previous models is that the non-linear TELM model calculates additional conductive and convective fluxes which appear when ballooning modes are destabilized.

3. Key factors limiting energy and particle losses in Type I ELMs. Small ELMs regimes

In spite of the fact that the present status of ELM theory cannot predict the size of the ELMs there are at least a number of theoretical suggestions of how to decrease the ELM affected pedestal volume. In particular the beneficial effects of high triangularity, high safety factor, high β_p in increasing of edge magnetic shear and decreasing the ELM affected area were largely discussed in the recent literature [36,38–40,45,4,46]. On the other hand the improved edge stability at high triangularity usually leads to a higher maximum achievable density in these regimes ($n/n_{GR} \sim 0.8-1$). The density increase plays an indirect role in the edge stability, first in decreasing characteristic diffusion time and the edge bootstrap current [36,45,41] and second, leading to the increased transport in ETB [45,4]. The comparison of the experimentally identified ELM affected area [47,10], and calculated eigenmodes width are correlated in DIII-D [36], JT-60U [38], AUG [40] and JET [48]. However the ELM size is not linked to the eigenmodes width in a simple way since there are many experimental examples when the ELM energy losses varies by factor of 3 while the ELM affected area is unchanged [48]. The separation of convective ($\sim \Delta n^{ELM}\,T$) and conductive($\sim \Delta T^{ELM} n$) energy losses in Type I ELMs [47] demonstrated similar dependences on plasma parameters and magnetic configurations in many tokamaks [10,48,49,42]. In particular it was shown that the conductive losses decrease strongly with the pedestal density while the particle convective loss fraction remains almost constant [49,10]. The other important factor decreasing conductive losses is high edge safety factor. Small ($\Delta W_{ELM}/W_{ped} \sim <5\%$) convective ELMs were demonstrated in JET at high ITER-like triangularity ($\delta \sim 0.5$) and high $q_{95} > 4.5$ even at low collisionality: $\nu^* \sim 0.06$ (Fig. 1). The theoretical explanation of the different dependence of convective and conductive losses on plasma parameters is still missing. However such plasmas have rather low collisionality ($\nu^* = 0.07-0.16$) and high confinement ($H_{98y2} \sim 1$) Grassy ELM regimes that are observed at high $\delta \sim 0.55$ and high $q_{95} > 6$ in JT-60U [12] could be the manifestation of the same trend in Type I ELM behaviour seen in strong edge shear configurations. The specific feature of the benign ELM regimes is the increased level of density and magnetic fluctuations characterized by a broadband frequency spectrum (<30 kHz) [13,39,14]. This suggests the existence of a mechanism increasing the transport through the ETB [14]. For example the high-n toroidal mode number ideal ballooning modes [46], or resistive Washboard modes, are proposed as a Type II ELMs mechanism [50].

There are H-modes without Type I ELMs at high pedestal collisionality ($\nu^* > 1$–5), such as the EDA regime observed in Alcator-C-Mod [15], High Recycling Steady (HRS) regime in JFT-2M [16], small ELMs in NSTX [51]. Such high collisionality regimes are hardly achievable in present machines and even less in ITER ($\nu^* \sim 0.05$). A common feature of H-modes without

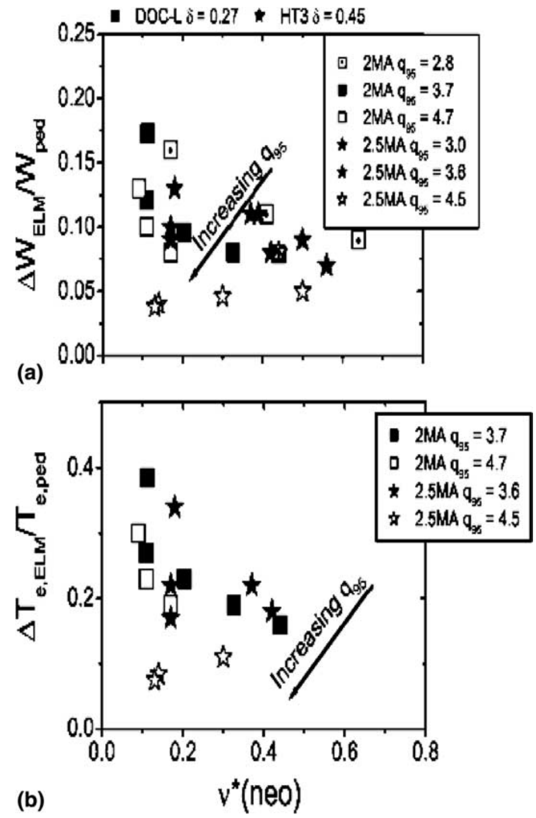

Fig. 1. (a) Normalized ELM energy loss to the pedestal energy versus pedestal plasma collisionality for different q_{95} in JET for medium and high triangularity (δ). The ELM energy loss is smaller for higher $\delta = 0.45$ and higher $q_{95} = 4.5$. (b) Normalized pedestal electron temperature drop in the ELM versus pedestal plasma collisionality in the same scans. Figures from [48].

ELMs is edge MHD activity as observed in EDA and HRS in the form of a quasi-coherent (QC) mode. This mode was associated with a resistive ballooning instability according to stability calculations, for example as done for Alcator-C-Mod [52].

A low collisionality $\nu^* \sim 0.05$ Quiescent H-mode (QH) without ELMs was first observed in DIII-D [17,20] and reproduced in AUG [3] as well as JT-60U [53]. Plasma shaping is not very important in this regime, but there are a number of other specific conditions. In particular, a high upper clearance configuration, low density (0.1–$0.4\, n_{GR}$ depending on the machine) and counter (opposite to the plasma current direction) neutral beam injection are required for QH regime. The resulting poor particle confinement and high $Z_{eff} \sim 3.3$–5 are the most common features for these regimes. The presence of the of the edge harmonics oscillation (EHO) is also a significant feature. All H-modes with benign small ELMs discussed above support the idea that in certain conditions the pedestal transport can be self-organized in a form of continuous MHD and turbulent activity sufficiently small so as not to loose the high confinement H-mode but at the same time resulting in avoidance of large Type I ELMs crashes.

4. External mechanisms of Type I ELMs control

According to the present knowledge, none of the benign ELM regimes discussed above seem directly applicable for ITER, but their physics suggest new ideas for external control mechanisms mainly based on the pedestal pressure and current profiles control.

4.1. Stochastic boundary

It is known that a small resonant ($q_{res} = m/n$) magnetic perturbation from control coils can create a stochastic layer in the plasma, where the perpendicular diffusion can be effectively increased by the diffusive-like behaviour of the magnetic field lines [54,55]. The transport in a stochastic magnetic field was largely studied mostly in circular machines [56–58]. The application of ergodic fields in H-modes in COMPASS-D [22] demonstrated the transition from ELM-free to ELMy regime (possibly Type III) when the radial magnetic perturbation was applied. An edge density and temperature decrease was observed, confirming the interpretation of

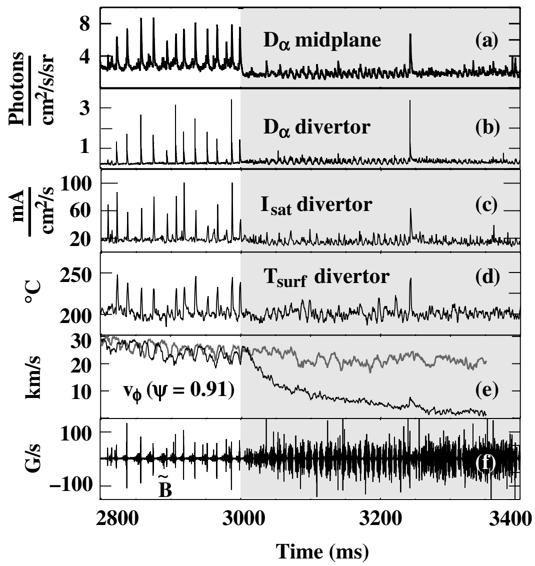

Fig. 2. ELM suppression during discharge 115467 in DIII-D using stochastic boundary created by the I-coil perturbation. (a) D_α from midplane and lower divertor, (b) particle flux to a Langmuir probe, (c) the surface temperature from an IR camera, (d) in the lower divertor. The edge toroidal rotation (e), (f) Mirnov signal. The shaded region indicates when the I-coil is on with current 4.4 kA. Figures from [25].

increased transport in the stochastic layer. The almost complete suppression of Type I ELMs in high triangularity H-modes was demonstrated in DIII-D at constant confinement [25] (see Fig. 2). The external magnetic perturbation from the internal coils (I-coils) (I_{coil} = 4.4 kA), mainly with toroidal number n = 3, was used. The effect was demonstrated in the range of q_{95} = 3.5–4 confirming its resonant nature. The electron pressure profile is unchanged as compared to Type I ELMs probably indicating only marginally increased transport in the ETB, but the recycling level for C^{IV} is increased with the ergodic field. The increased level of edge MHD was observed while the I-coil perturbation was applied. The observed decrease of the toroidal plasma rotation (Fig. 2(e)), which was expected in the presence of the static perturbation applied at the edge, did not perturb the H-mode in present experiments.

4.2. Pellets

The control of the ELM frequency and size by pellets was intensively studied on AUG [26]. The fact that pellets usually trigger an ELM was known from plasma fuelling experiments. The product of ELM frequency and averaged energy loss from an ELM is roughly constant in most H-mode experiments in many tokamaks [59] apart from some exceptions at high triangularity or high collisionality [39]. This general experimental observation suggest that increasing ELM frequency leads to smaller ELMs, but at the same time to plasma confinement degradation. One possible way to break this link is to control ELM frequency and ELM size independently. This was done for example in pellet ELM control experiments in AUG. The aim of ELM control by pellets is to trigger ELMs with given size, but to avoid over-fuelling of the main plasma and decreasing the global confinement. It was demonstrated [26] that the injection of small ($\sim$1.4 mm^3, $\sim 6.10^{19}$ D-atom, V $\sim$ 560 m/s, High Field Side) pellets can trigger ELMs with the pellet injection frequency f_{pellet} if the natural Type I ELM frequency, $f_{intrinsic} < f_{pellet}$ (Fig. 3). Increasing f_{pellet} imposes refuelling and confinement degradation, but with weaker plasma diamagnetic energy dependence on ELM frequency: $W_{MHD} \sim f_{ELM}^{-0.16}$ as opposed to the experimental scaling with gas puff in AUG, $W_{MHD} \sim f_{ELM}^{-0.6}$ (Fig. 3). The electron pressure profiles (however lower gradients were observed for pellets), magnetic signature, heat loads on the divertor plates of pellet triggered ELMs are all very close to the intrinsic ELMs with similar frequency [26]. This probably suggests that triggered ELMs have the same nature as destabilized MHD modes. The pedestal collisionality is usually increased by pellets [26]. The modelling of the possibility of controlling ELMS using pellets to increase the pedestal collisionality in ITER has been done in [60].

4.3. Edge current and electromagnetic ELM triggering

Another control tool suggested by ideal MHD stability theory is the edge current density [37,35,36,41]. The possibilities to change edge current are limited in present machines since reliable current drive techniques are not known at the plasma edge. However, the edge current can be changed in current ramp experiments since the resistive time ($\sim T_e^{-3/2}$) at the edge is much lower then in the plasma centre, leading to the local increase and

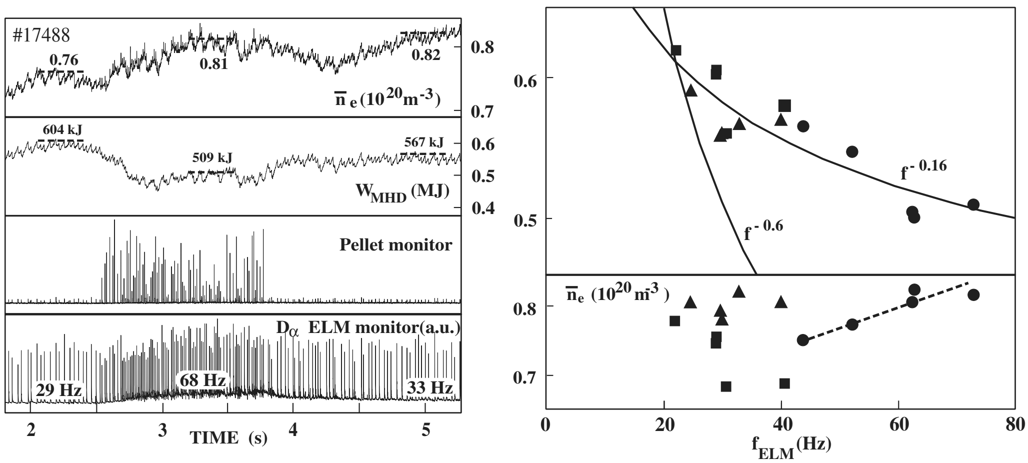

Fig. 3. (Left) Density, diamagnetic energy, pellet monitor and Dα signals during external gas puff without pellets (f_{ELM} = 29 Hz), small pellets and no puff (f_{ELM} = 68 Hz) and with external puff only (f_{ELM} = 68 Hz). (Right) Diamagnetic energy and line averaged electron density dependence on ELM frequency without gas(squares), gas puffed(triangles) and pellet phases (circles). Increasing f_{pel} imposes slight refuelling and confinement degradation. A fit to data with pellets: $W_{MHD} \sim f_{ELM}^{-0.16}$. Experimental scaling with gas puff in AUG $W_{MHD} \sim f_{ELM}^{-0.6}$. Figures from [62].

decrease of the parallel current density in ramp-up and down phase respectively. Edge current can play a stabilising role giving access to the second stability regime for ballooning modes, but further increase of the edge current density can destabilise low n-peeling modes. [4,7]. Current ramp experiments confirmed the main trends given by ideal MHD stability theory. However the possibility of ramping current (and in particular time derivation dI_p/dt) usually is limited by technical limits specific for each machine. Depending also on the resistive time, the plasma response can be rather slow (~ 0.5 s in JET [4,7]).

More rapid changes of edge current density is possible using the technique of vertical displacements of the plasma column, first done in COMPASS-D [22], and more recently in TCV with vertical control coils [27]. It was demonstrated that ELM frequency locks to the frequency of these oscillations. At present these ELMs are interpreted as a manifestation of a peeling instability occurring periodically due to the periodic changes in the edge current density. First optimistic estimations of such a technique for ELM control in ITER using external poloidal coils have been done [27] but further experimental investigations on larger tokamaks are required and, in particular, the study of the plasma confinement in such regimes. In particular, recent similar AUG experiments demonstrated that Type I ELMs are preferentially triggered when plasma column moves downwards to the divertor meaning at lower edge current density which is opposite to TCV results [61]. The possible explanation can be in the different stability and collisionality regimes in the machines. If such pedestal parameters as pressure gradient and current are close to the high n ballooning stability limit the decrease of edge current density could trigger Type I ELMs (as in AUG). If the pedestal pressure is low (as in TCV) and the pedestal parameters are close to the low n peeling limit the increased edge current density could lead to the triggering of Type III ELMs. Further experiments and stability analysis should be done before any extrapolation of this ELM control method for ITER.

5. Conclusions

The destabilisation of ballooning and peeling modes in the region of steep edge gradients in H-mode is largely supported by experimental data as a triggering mechanism at least for Type I ELMs. The present status of the modelling does not permit self-consistent calculations of energy and particle losses in ELMs. Nevertheless, both theory and experiment suggest the benefit of high plasma shaping (triangularity), high q_{95}, and high pedestal density on the reduction of the size of Type I ELMs.

In particular the most important conductive part of energy lost during the ELM decreases strongly with density (collisionality) and also at high q_{95}, leading to the small ($\Delta W_{\mathrm{ELM}}/W_{\mathrm{ped}} < 5\%$) convective ELMs.

Small benign ELMs regimes (EDA, HRS, Type V, Type II, Grassy, QH) were demonstrated in present machines in very specific conditions regarding magnetic configuration and pedestal parameters, and are not applicable directly to ITER.

Active control of Type I ELMs is progressing in present tokamaks. The possibility of almost complete Type I ELMs suppression, by edge ergodisation at constant confinement, was demonstrated in DIII-D. ELM frequency and size can be controlled by small pellets (AUG), minimising confinement degradation due to fuelling as compared to gas injection. The experiments on TCV and AUG demonstrated the possibility of locking the ELM frequency to the frequency of rapid vertical plasma oscillations induced by position control coils. For the moment active control ELM tools are in the stage of the demonstration of the main principle followed by a study of the underlying physics. Further investigations will identify the applicability of these methods to Type I ELM control in ITER.

References

[1] H. Zohm, Plasma Phys. Control. Fus. 38 (1996) 105.
[2] J.W. Connor, Plasma Phys. Control. Fus. 40 (1998) 531.
[3] W. Suttrop, Plasma Phys. Control. Fus. 42 (2000) A1.
[4] M. Becoulet et al., Plasma Phys. Control. Fus. 45 (2003) A93.
[5] G. Saibene et al., Nucl. Fus. 39 (1999) 1133.
[6] L.D. Horton, Nucl. Fus. 39 (1999) 1.
[7] R. Sartori et al., Plasma Phys. Control. Fus. 46 (2004) 723.
[8] B.J. Green for the ITER Int. Team, Plasma Phys. Control. Fus. 45 (2003) 687.
[9] G. Federici et al., Plasma Phys. Control. Fus. 45 (2003) 1523.
[10] A. Loarte et al., Plasma Phys. Control. Fus. 45 (2003) 1549.
[11] J. Rapp et al., Nucl. Fus. 44 (2004) 312.
[12] Y. Kamada et al., Plasma Phys. Control. Fus. 42 (2000) A247.
[13] J. Stober et al., Nucl. Fus. 41 (2001) 1123.
[14] G. Saibene et al., Plasma Phys. Control. Fus. 44 (2002) 1769.
[15] A. Hubbard et al., Phys. of Plasmas 8 (2001) 2033.
[16] K. Kamiya et al., Plasma Phys. Control. Fus. 46 (2004) A157.
[17] K.H. Burrell et al., Plasma Phys. Control. Fus. 44 (2002) A253.
[18] T. Fujita, Plasma Phys. Control. Fus. 44 (2002) A19.
[19] Y. Kamada et al., Plasma Phys. Control. Fus. 44 (2002) A279.
[20] P. Gohil, Plasma Phys. Control. Fus. 44 (2002) A37.
[21] A.C. Sips et al., Plasma Phys. Control. Fus. 44 (2002) A151.

[22] S.J. Fielding, R.J. Buttery, et al., Proceedings 2001 EPS Conf., ECA 25A (2001) 1825.
[23] H. Tamai et al., J. Nucl. Mater. 200–222 (1995) 365.
[24] R. A Moyer, T.E. Evans, EPS Conf. on Plasma Phys. Contr. Fus. Montreux 26B, 2002, P-1.063.
[25] T. Evans et al., Phys. Rev. Lett. 92 (2004).
[26] P.T. Lang et al., Nucl. Fus. 43 (2003) 1110.
[27] A.W. Degeling et al., Plasma Phys. Control. Fus. 45 (2003) 1637.
[28] N. Oyama et al., Nucl. Fus. 43 (2003) 1250.
[29] N. Oyama et al., Nucl. Fus. 44 (2004) 582.
[30] I. Nunes et al., Proc 2003 EPS Conf., ECA, vol. 27A, 2003, P-1.157.
[31] A. Loarte et al., Plasma Phys. Control. Fus. 44 (2002) 1815.
[32] G.F. Counsell et al., Plasma Phys. Control. Fus. 44 (2002) 827.
[33] J. Boedo et al., J. Nucl. Mater., these Proceedings, doi:10.1016/j.jnucmat.2004.10.159.
[34] A. Kirk, Phys. Rev. Lett. 92 (2004) 245002.
[35] H.R. Wilson et al., Phys Plasmas 9 (2002) 1277.
[36] P.B. Snyder et al., 'ELMs and constrains on the H-mode pedestal: a model based on peeling-ballooning modes', in: Proceedings of the 19th Int. conference, Lyon, 2002, Vienna: IAEA.
[37] G.T.A. Huysmans et al., Nucl. Fus. 38 (1998) 179.
[38] L.L. Lao, Plasma Phys. Control. Fus. 42 (2000) A51.
[39] M. Becoulet et al., Plasma Phys. Control. Fus. 44 (2002) A103.
[40] S. Saarelma et al., Nucl. Fus. 43 (2003) 262.
[41] J. Lönnroth et al., Plasma Phys. Control. Fus. 46 (2004) A249.
[42] S. Cowley et al., Plasma Phys. Control. Fus. 45 (2003) A31.
[43] X. Xu et al., New J. Phys. 4 (2002) 53.1.
[44] Yu. Igitkhanov et al., A Physics Picture of Type I ELMs 28th EPS Conf. Control. Fus. Plasma Phys., 2001, Contr. No. P-4.101.
[45] V. Parail et al., 28th EPS Conf. on Plasma Phys. Control. Fus., Madeira, 25A, 2001, P-5.027.
[46] J. Lönnroth et al., Plasma Phys. Control. Fus. 46 (2004) 767.
[47] A.W. Leonard et al., Plasma Phys. Control. Fus. 44 (2002) 945.
[48] A. Loarte et al., Phys. Plasmas 11 (2004) 2668.
[49] A.W. Leonard et al., J. Nucl. Mater. 313–316 (2003) 768.
[50] C.P. Perez et al., Plasma Phys. Control. Fus. 46 (2004) 61.
[51] R. Maingi et al., J. Nucl. Mater., these Proceedings, doi:10.1016/j.jnucmat.2004.08.023.
[52] D.A. Mossessian, 'H-mode edge stability of Alcator C-mod plasmas' in: Proceedings of the 19th Int. conference, Lyon, 2002, EX/P5-04, Vienna: IAEA.
[53] Y. Sakamoto et al., Plasma Phys. Control. Fus. 46 (2004) A299.
[54] A.B. Rechester, M.N. Rosenbluth, Phys. Rev. Lett. 40 (1978) 38.
[55] A. Samain et al., Phys. Fluids B 5 (1993) 471.
[56] P. Ghendrih et al., Plasma Phys. Control. Fus. 38 (1996) 1653.
[57] S.C. McCool et al., Nucl. Fus. 29 (1989) 547.
[58] M. Lehnen et al., J. Nucl. Mater., these Proceedings, doi:10.1016/j.jnucmat.2004.10.100.
[59] A. Herrmann et al., Plasma Phys. Control. Fus. 44 (2002) 883.
[60] A.R. Polevoi et al., Nucl. Fus. 43 (2003) 1072.
[61] P.T. Lang et al., 31st EPS Conference on Plasma Phys. London, 28th June–2nd July 2004, ECA, vol. 28B, P-4.135.
[62] P.T. Lang et al., 30th EPS Conference on Contr. Fus. Plasma Phys., Russia, St. Petersburg, 2003, ECA, vol. 27A, P. 1.129.